

olis interaction admix such 2-qp to 0-qp states appreciably. (ii) Only if the Fermi level is near to the level in question can it contribute strongly.

In our calculations of the Pt and Hg isotopes additional contributions have been calculated and are found to be small. This is obviously because in these nuclei the 2-qp states ( $\nu i_{13/2}$  and  $\pi h_{11/2}$ ) are the only high- $j$  levels near the Fermi surface.

We thank Professor H. J. Mang, Professor V. Madsen, Dr. K. Goeke, Dr. K. W. Schmid, and Dr. K. Shimizu for numerous enlightening discussions. Our collaboration with Professor P. Vogel and Dr. K. Neergard in the study of negative-parity states of even-even mass nuclei has been of immense help in the present investigation.

<sup>1</sup>C. Günther, H. Hübel, A. Kleinrahm, D. Mertin, B. Richter, W. D. Schneider, and R. Tischler, Phys. Rev. C **15**, 1298 (1977).

<sup>2</sup>D. Proetel, F. S. Stephens, and R. M. Diamond, in *Proceedings of the International Conference on Reactions between Complex Nuclei, Nashville, Tennessee, 1974*, edited by R. L. Robinson, F. K. McGowan, J. B.

Ball, and J. H. Hamilton (North-Holland, Amsterdam, 1974), p. 162.

<sup>3</sup>H. Beuscher, W. F. Davidson, R. M. Lieder, and A. Neskakis, Phys. Rev. Lett. **32**, 843 (1974).

<sup>4</sup>M. Piiparinen, J. C. Cunnane, P. J. Daly, C. L. Dors, F. M. Bernthal, and T. L. Khoo, Phys. Rev. Lett. **34**, 1110 (1975), and references on earlier experiments contained therein.

<sup>5</sup>S. A. Hjorth, A. Johnson, Th. Lindblad, L. Funke, P. Kemnitz, and G. Winter, Nucl. Phys. **A262**, 328 (1976), and references on earlier experiments contained therein.

<sup>6</sup>F. S. Stephens and R. Simon, Nucl. Phys. **A183**, 257 (1972); F. S. Stephens, Rev. Mod. Phys. **47**, 43 (1975).

<sup>7</sup>M. S. Mariscotti, G. Scharff-Goldhaber, and B. Buck, Phys. Rev. **178**, 1864 (1969).

<sup>8</sup>H. Toki and A. Faessler, Z. Phys. **A276**, 35 (1976).

<sup>9</sup>B. Banerjee, H. J. Mang, and P. Ring, Nucl. Phys. **A215**, 366 (1973); K. W. Schmid *et al.*, Phys. Lett. **63B**, 399 (1975); A. Faessler *et al.*, Nucl. Phys. **A256**, 106 (1976).

<sup>10</sup>H. Toki, K. Neergard, P. Vogel, and A. Faessler, Nucl. Phys. **A279**, 1 (1977).

<sup>11</sup>C. Flaum and D. Cline, Phys. Rev. **14**, 1224 (1976).

<sup>12</sup>A. Faessler, W. Greiner, and R. K. Sheline, Nucl. Phys. **62**, 241 (1965).

## $^{12}\text{C}(e, e'\pi^+)$ Reaction Leading to Low-Lying States in $^{12}\text{B}$

K. Shoda, H. Ohashi, and K. Nakahara

Laboratory of Nuclear Science, Tohoku University, Tomizawa, Sendai 982, Japan

(Received 21 July 1977)

Energy and angular distributions of photopions from  $^{12}\text{C}$ , leading to low-lying residual states in  $^{12}\text{B}$ , have been measured via the  $(e, e'\pi^+)$  reaction at  $E_e = 195$  MeV. The shape of the patterns agrees with the theoretical estimates deduced from other electron scattering data and also with shell-model calculations. A comparison of the absolute value shows the importance of correct estimation of the pion wave. The result demonstrates that photopion experiments can provide a promising method for studying spin-flip-type electromagnetic transitions in nuclei.

It is well known that the photopion production from a nucleon is caused mainly by a spin-flip-type transition, the leading term of the amplitude of this transition being proportional to  $\vec{\sigma} \cdot \vec{\epsilon}$ , where  $\vec{\sigma}$  is the intrinsic spin operator of nucleon and  $\vec{\epsilon}$  is the photon polarization vector.<sup>1</sup> When only the leading term is applied to express the photopion cross section of complex nuclei, the cross section is given in the impulse approximation by

$$\left(\frac{d\sigma}{d\Omega}\right)_{\gamma\pi} = \frac{p_\pi}{km_\pi^2} e^2 f^2 \frac{1}{J_i^2} \sum_{M_i} \sum_{M_f} |\vec{\epsilon} \cdot \vec{\mathfrak{M}}|^2, \quad (1)$$

$$\vec{\mathfrak{M}} = \langle J_f M_f | \sum_{n=1}^A \vec{\sigma}_n \tau_n^\pm \exp(i\vec{q} \cdot \vec{r}_n) | J_i M_i \rangle, \quad (2)$$

where  $k$  and  $p_\pi$  are the momenta of the incident

photon and the outgoing pion, respectively,  $m_\pi$  is the pion rest mass,  $e^2 = \frac{1}{137}$ ,  $f^2 = 0.08$ ,  $\hat{J} \equiv (2J + 1)^{1/2}$ ,  $J$  and  $M$  are nuclear spin and magnetic quantum number with suffix  $i$  or  $f$  denoting the initial or final state, respectively,  $\tau^\pm$  is the isospin raising and lowering operator,  $\vec{q} = \vec{k} - \vec{p}_\pi$  is the nuclear recoil momentum,  $\vec{r}_n$  is position vector of a component nucleon,  $|J_i M_i\rangle$  and  $|J_f M_f\rangle$  are the initial and final nuclear states, respectively, and  $\sum_{S\gamma}$  means summation over the photon polarization.<sup>2,3</sup>

As shown by Eqs. (1) and (2), photopion cross sections on complex nuclei are expressed in terms of the matrix element  $\vec{\mathfrak{M}}$  of the nuclear spin-flip-type charge-exchange electromagnetic transition of a momentum transfer  $\vec{q}$ . On the ba-

sis of the relation between the isospin operators  $\tau^\pm$  and  $\tau_3$ ,  $\vec{\tau}$  can be related to the electromagnetic transition between the isobaric analog states and the ground state in the target nucleus. Überall and co-workers<sup>2,3</sup> proposed a method to estimate photopion cross sections from the electron scattering data after rotation in isospin space so as to change the isospin operator in Eq. (2) from  $\tau^\pm$  to  $\tau_3$ . They calculated the photopion cross section of  $^{12}\text{C}$  by this method using parameters obtained by the Helm model fitted to the electron scattering data which have been studied particularly well. The present report discusses the experimental results for the reaction  $^{12}\text{C}(e, e'\pi^+)^{12}\text{B}$ , making a comparison both with their estimate and with shell-model calculations.<sup>2-5</sup>

Energy and angular distributions have been measured for positive pions emitted from the reaction  $^{12}\text{C}(e, e'\pi^+)$  using a 195-MeV (total energy) electron beam from the Tohoku University linear accelerator. Emitted particles were momentum analyzed with a 169.7° deflecting magnetic spectrometer and detected with a 33-channel detector array on the focal plane. Each channel is composed of a triple coincidence system of Si(Li) solid state detectors along the direction of the incident particles in order to reduce background counts. Pions were discriminated from background positrons by the discriminator bias setting as shown in Fig. 1. All charged nuclear particles were stopped in the first detector of the coincidence system. The target was a natural carbon plate of thickness 184 mg/cm<sup>2</sup>. The angle between the incident electron beam and the target plane was adjusted for best pion energy resolution. The overall energy resolution in the experiment was 0.52–0.46 MeV full width at half-maximum (FWHM) at detection angles with respect to

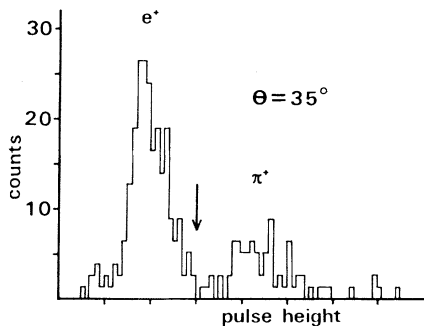


FIG. 1. An example of pulse height distribution from a Si(Li) solid-state detector in triple coincidence. An arrow indicates the discriminator bias setting.

the incident beam of  $\theta = 30^\circ$ – $110^\circ$ , and 1.6 and 1.4 MeV at  $\theta = 130^\circ$  and  $150^\circ$ , respectively. The pion counts were corrected for decays that occur during passage through the apparatus. The effect of the bremsstrahlung produced at the target was neglected since it is small in the case of light nuclei.

The pion energy distributions for the  $(e, e'\pi^+)$  reaction are shown in Fig. 2. The error bars show statistical errors only. On the basis of the virtual-photon theory,<sup>6</sup> the interaction between a high-energy electron and the nucleus can be described by means of a virtual photon; the pion energy distribution leading to a residual state is expressed in terms of the  $(\gamma, \pi)$  cross section and the virtual-photon spectrum  $N_{h\nu}(E_e, E_\gamma)$  associated with an electron of energy  $E_e$  as

$$\frac{d^2\sigma_{(e, e'\pi)}(T_\pi, E_R)}{d\Omega dT_\pi} = \frac{d\sigma_{(\gamma, \pi)}(E_\gamma, E_R)}{d\Omega} N_{h\nu}(E_e, E_\gamma). \quad (3)$$

Here  $T_\pi$  is the pion kinetic energy. In the frame-

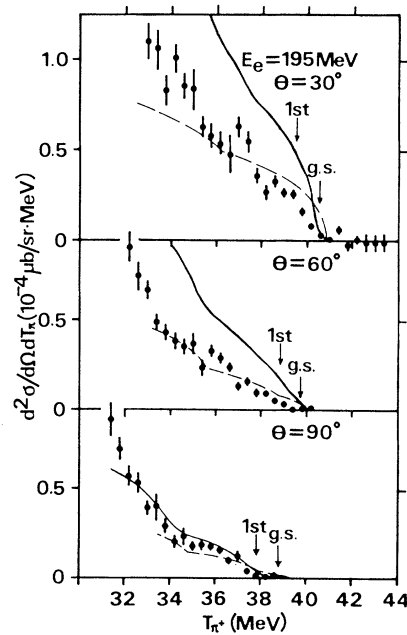


FIG. 2. Pion energy distribution in  $^{12}\text{C}(e, e'\pi^+)^{12}\text{B}$ . Solid curves are the theoretical estimates derived from Eqs. (3) and (4) and the Helm model using the electron scattering data (Refs. 2 and 3). Dashed curves are the theoretical result with a nuclear shell-model and pion wave with Coulomb correction (Ref. 5). Arrows indicate the maximum energy of pion leading to the ground- and first excited residual states.

work of the laboratory system,  $T_\pi$  is determined from the photon energy  $E_\gamma$ , the residual energy  $E_R$ , the threshold value, and the detection angle of the pion. When photopions lead to several residual states, the pion energy distribution is given by Eq. (3) summed over these states:

$$\frac{d^2\sigma_{(e,e'\pi)}(T_\pi, E_R)}{d\Omega dT_\pi} = \sum_{E_R} \frac{d\sigma_{(\gamma,\pi)}(E_\gamma, E_R)}{d\Omega} N_{h\nu}(E_e, E_\gamma). \quad (4)$$

In the present experiment, scattered electrons  $e'$  were not detected. In this case the result relates to the electrons scattered into all directions. As is well known, electron scattering is extremely strong in the forward direction. Therefore the result can be approximated with the case of scattering into the same direction as incidence ( $\theta = 0^\circ$ ) where the momentum transfer to the nucleus is equal to the case of the real photon. The virtual-photon spectra were calculated in the distorted-wave Born approximation by Gargaro and Onley.<sup>7</sup> On the light nuclei, their result shows no remarkable difference from the result calculated in the plane-wave approximation.

The solid curves in Fig. 2 are the pion energy distributions calculated from Eq. (4). In this calculation, the  $(\gamma, \pi^+)$  cross sections were obtained by the same method as in Refs. 2 and 3, and the virtual-photon spectrum was calculated in the plane-wave approximation.<sup>8</sup> The result was smeared out corresponding to the energy resolution of the experiment.

Recently Furui<sup>5</sup> calculated the  $(e, e'\pi^+)$  cross sections in the one-photon exchange approximation; a nuclear shell model normalized properly was used and the Coulomb correction for the pion was taken into account. The result is shown by the dashed curves in Fig. 2.

In order to measure the photopion angular distributions, the energy distributions of pions produced in the  $(e, e'\pi^+)$  reaction have been measured at angles  $\theta = 30^\circ - 150^\circ$  in steps of  $10^\circ$  or  $20^\circ$ . The pion energy distribution within about 1 MeV of the maximum energy pions contributes only to the reaction leaving the residual nucleus in its ground state since the first excited state is at 0.95 MeV. Therefore the  $(\gamma, \pi^+)$  cross sections for the residual nuclei  $^{12}\text{B}$  being left in its ground state ( $1^+$ ) were obtained from the  $(e, e'\pi^+)$  spectra using Eq. (3) with the virtual-photon spectrum. Similarly the  $(\gamma, \pi^+)$  cross sections for the first excited residual state ( $2^+$ ) were calculated from the

pion energy distributions corresponding to this state and the ground state. The contribution from the ground-state transition was subtracted by extending the spectrum from the uppermost energy region. The photon energy effective in the present analysis is about 194 MeV. The absolute value of the experimental  $(\gamma, \pi^+)$  cross sections was checked with the measurement of the  $\text{H}(e, e'\pi^+)$  reaction cross section using a LiH target at  $E_\lambda \approx 180$  MeV and  $\theta = 30^\circ$ ; the cross section of  $\text{H}(\gamma, \pi^+)$  was calculated from this result by the same method as for  $^{12}\text{C}$ . The result is  $7.28 \pm 0.45 \mu\text{b}/\text{sr}$  and is in good agreement with the previous result.<sup>9</sup>

The experimental angular distributions are shown in Fig. 3 together with the estimate calculated by the method of Überall and co-workers<sup>2,3</sup> and that from the shell-model theory<sup>4</sup> which was calculated for  $E_\gamma = 200$  MeV and assumed approximately equal in the case of the present energy. The experimental data at  $\theta = 130^\circ$  and  $150^\circ$  possibly include a contribution from the second excited state ( $E_R = 1.67$  MeV) in  $^{12}\text{B}$  because of poor energy resolution; this contribution is about 35% of the data if the ratio of the theoretical cross sections<sup>2,3</sup> for the first and second excited states in

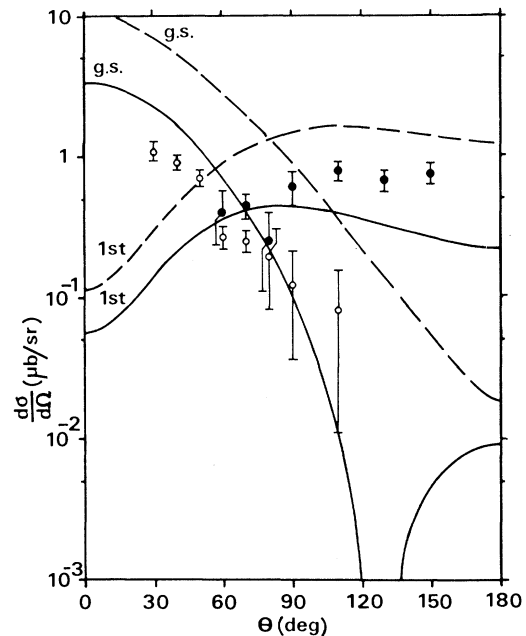


FIG. 3. Pion angular distributions in  $^{12}\text{C}(\gamma, \pi^+)^{12}\text{B}$  at  $E_\gamma \approx 194$  MeV leaving the ground state (open circles) and the first excited state (closed circles) in  $^{12}\text{B}$ . Solid curves and dashed curves are the theoretical estimates by the Helm model using electron scattering data (Refs. 2 and 3) and by the shell model (Ref. 4), respectively.

TABLE I. Comparison of cross sections of the  $^{12}\text{C}(\gamma, \pi^+)^{12}\text{B}$  reaction relating to the ground and first excited residual states.  $R$  is the most probable value of the ratio  $(d\sigma/d\Omega)_{\text{expt}}/(d\sigma/d\Omega)_{\text{theor}}$ .  $\sigma_{\text{expt}}$  is calculated from  $\sigma_{\text{theor}}$  multiplied by  $R$ .

Residual state	Ground state ( $J^\pi = 1^+$ )	First excited state ( $E_R = 0.95 \text{ MeV}, J^\pi = 2^+$ )
Helm model theory <sup>a</sup>		
$R$	$0.56 \pm 0.03$	$1.42 \pm 0.13$
$\sigma_{\text{theor}} (\mu\text{b})$	27.04	16.55
$\sigma_{\text{expt}} (\mu\text{b})$	$15.1 \pm 0.8$	$23.5 \pm 2.3$
Shell-model theory <sup>b</sup>		
$R$	$0.14 \pm 0.01$	$0.43 \pm 0.04$
$\sigma_{\text{theor}} (\mu\text{b})$	99.9	59.5
$\sigma_{\text{expt}} (\mu\text{b})$	$14.0 \pm 1.0$	$25.6 \pm 2.4$

<sup>a</sup>Refs. 2 and 3.

<sup>b</sup>Ref. 4.

$^{12}\text{B}$  is used.

Table I shows the most probable values of the ratio between the experimental and theoretical angular distributions in the range of angles measured. The theoretical cross sections are obtained by integrating the theoretical angular distributions, and experimental ones are estimated from the theoretical cross sections multiplied by the ratio mentioned above; both results are also shown in Table I. The present data are in better agreement with the theory based on electron scattering than with the shell-model theory. The overestimate of the absolute value in the shell-model theory as shown in Table I is similar to the cases for other processes such as electron scattering, muon capture, and  $\beta$  decay.<sup>4</sup> The former theory is close to a surface-production model, because the nuclear transition density of the Helm model is concentrated on the nuclear surface; in contrast to that, the latter is a volume-production model.

The absorption and distortion of photopions in nuclei was calculated by Cannata *et al.* using an optical potential.<sup>3</sup> They found that  $s$ -wave pion production is suppressed and  $p$ - or  $d$ -wave production is enhanced in the theoretical cross sections calculated from the electron scattering data. If the photopions are emitted after dipole photoabsorption in  $^{12}\text{C}$ , the pions leaving  $^{12}\text{B}$  in the ground state ( $1^+$ ) and the first excited state ( $2^+$ ) should be emitted as mainly  $s$  wave and as mainly  $p$  or  $d$  wave, respectively. This prediction by Cannata *et al.* qualitatively improves the agreement between experiment and the Helm model estimate (see Table I). The pion spectra calculated by Furui<sup>5</sup> with the Coulomb correction for

the pion agree well with the present experimental result as shown in Fig. 2. This also suggests the importance of correct estimation of the pion wave.

As shown in Eqs. (1) and (2), studies of photopion production will give information about spin-flip-type electromagnetic transition strengths to the upper isospin state ( $\Delta T = 1$ ). These transitions are usually weak in nuclear reactions and difficult to measure, because the corresponding interaction is of second order and a large background arises from strong transitions to the lower isospin states ( $\Delta T = 0$ ) which have a high level density. The present result indicates that photopion experiments can provide a good method of deducing the spin-flip-type electromagnetic transition strengths in nuclei without suffering from the large background. A more precise calculation of pion absorption in nuclei would, however, be useful in a more detailed interpretation of the present experimental results.

<sup>1</sup>G. F. Chew, M. L. Goldberger, F. E. Low, and Y. Nambu, Phys. Rev. **106**, 1345 (1957).

<sup>2</sup>H. Überall, B. A. Lamers, C. W. Lucas, and A. Nagl, Phys. Lett. **44B**, 324 (1973).

<sup>3</sup>F. Cannata, B. A. Lamers, C. W. Lucas, A. Nagl, H. Überall, C. Werntz, and F. J. Kelly, Can. J. Phys. **52**, 1405 (1974).

<sup>4</sup>J. B. Seaborn, V. Devanathan, and H. Überall, Nucl. Phys. **A219**, 461 (1974).

<sup>5</sup>S. Furui, private communication, and in Proceedings of the International Conference on High-Energy Physics and Nuclear Structure, Zürich, Switzerland, 29 August–2 September 1977 (to be published).

<sup>6</sup>R. H. Dalitz and D. R. Yennie, Phys. Rev. **105**, 1598 (1957).

<sup>7</sup>W. W. Gargaro and D. S. Onley, Phys. Rev. C 4, 1032 (1971).

<sup>8</sup>J. M. Eisenberg and W. Greiner, *Excitation Mechanism of the Nucleus* (North-Holland, Amsterdam, 1970).

<sup>9</sup>M. I. Adamovich, V. G. Larionova, A. I. Lebedev, S. P. Kharlamov, and F. R. Yagudina, in *Photomesic and Photonuclear Processes*, edited by D. V. Skobel'tsyn (Consultants Bureau, New York, 1967), p. 49.

## Evidence for a Rotational Band in <sup>24</sup>Mg and Its Fragmentation: A Rotation-Vibration Coupling?

N. Cindro,<sup>(a)</sup> F. Coçu, J. Uzureau, Z. Basrak,<sup>(a)</sup> M. Cates, J. M. Fieni, E. Holub,<sup>(a)</sup>  
Y. Patin, and S. Plattard

*Service de Physique Nucléaire, Centre d'Etudes Nucléaires Bruyères le Châtel, France*

(Received 26 July 1977)

Three resonances in <sup>12</sup>C + <sup>12</sup>C with  $E_{c.m.}(J^\pi)$  of 8.85(6<sup>+</sup>), 11.2(8<sup>+</sup>), and 13.75(10<sup>+</sup>) are reported. Together with earlier data, these resonances fit in a rotational band in <sup>24</sup>Mg. A model based on the rotation-vibration coupling is proposed to account for these data.

Several recent experiments<sup>1-4</sup> have provided new information on spins and parities of resonances in <sup>24</sup>Mg at high energies of excitation. In the present experiment, we investigate the reaction <sup>12</sup>C(<sup>12</sup>C,  $\alpha$ )<sup>20</sup>Ne in the range  $6.85 \leq E_{c.m.} \leq 15$  MeV and report three resonances at  $E_{c.m.} = 8.85$ , 11.2, and 13.75 MeV to which we assign definite  $J^\pi$  values. Combining these results with the data from previously reported measurements<sup>3</sup> and the results of other authors,<sup>1,2,4-9</sup> we attempt a unified picture of the resonances in <sup>24</sup>Mg.

The present experiment was performed using the Model FN tandem accelerator of the Centre d'Etudes Nucléaires Bruyères le Châtel.  $\alpha$  particles from the reaction <sup>12</sup>C(<sup>12</sup>C,  $\alpha$ )<sup>20</sup>Ne were momentum analyzed in a split-pole magnetic spectrograph and detected in position-sensitive detectors. The excitation functions of four  $\alpha$  groups leading to, respectively, the ground state and the 1.63-, 4.25-, and 4.97-MeV states in <sup>20</sup>Ne were measured at 10° and 20° using a 30- $\mu$ g/cm<sup>2</sup> carbon target. In addition, the ground-state excitation function was measured at 7.5° lab using a 50- $\mu$ g/cm<sup>2</sup> target. From the correlated maxima in the excitation functions of transitions leading to natural-parity states in <sup>20</sup>Ne and the relative smallness of the 2<sup>-</sup> excitation function at very forward angles, energies around  $E_{c.m.} = 8.85$ , 11.2, and 13.75 MeV were selected as likely candidates for resonances, and ground-state  $\alpha$  angular distributions were measured on and off these energies. For a narrow, noninterfering resonance of spin  $J=L$ , the angular distribution follows the form

$$\sigma(\theta) = A_L^2 P_L^2 |\cos\theta|^2 \quad (1)$$

or else (equivalently)

$$\sigma(\theta) = \sum_{l=0}^{l_{\max}=2L} a_l P_l(\cos\theta) \quad (l \text{ even}). \quad (2)$$

The comparison of the angular distributions at  $E_{c.m.} = 11.2$  and 13.75 MeV with the  $P_8^2(\cos\theta)$  and  $P_{10}^2(\cos\theta)$  shapes, respectively, is shown in Fig. 1; the agreement is quite satisfactory.

The measured angular distributions were subsequently submitted to a  $\chi^2(l_{\max})$  analysis using expression (2). The values of  $\chi^2$  plotted vs the maximal degree of polynomials used are shown

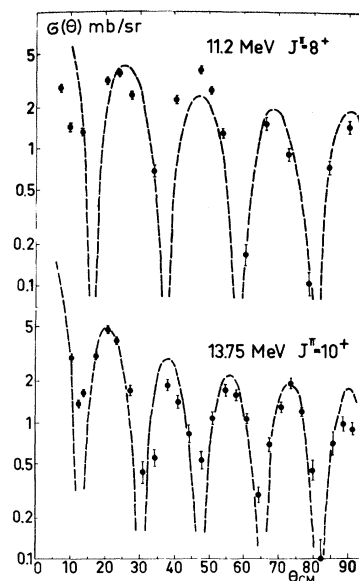


FIG. 1. The 11.2- and 13.75-MeV angular distributions compared with the  $P_8^2(\cos\theta)$  and  $P_{10}^2(\cos\theta)$  shapes, respectively.